

Effect of miR-129-3p on autophagy of interstitial cells of Cajal in slow transit constipation through SCF C-kit signaling pathway

Heng Wang^{1,2#}, Bingbing Ren^{1#}, Jun Pan^{3#}, Siqi Fu¹, Chunxiang Liu¹ and Daqing Sun¹✉

¹Department of Pediatric Surgery, Tianjin Medical University General Hospital, Tianjin 300052, China; ²Department of Gastrointestinal Surgery/ Pediatric Surgery, Renmin Hospital, Hubei University of Medicine, Shiyan, Hubei 442000, China; ³Department of Traditional Chinese Medicine, Renmin Hospital, Hubei University of Medicine, Shiyan, Hubei 442000, China

Objective: To explore the mechanism by which miR-129-3p affected the autophagy of interstitial cells of Cajal (ICCs) in slow transit constipation tissues through the SCF C-kit signaling pathway. **Methods:** Colon samples from 20 Slow transit constipation (STC) patients who underwent total colectomy plus ileorectal anastomosis or subtotal colon resection plus anti-peristaltic rectal anastomosis were collected in our hospital. The colon of 20 non-STC patients was used as control. The control of this study was 20 patients undergoing radical surgery for colon cancer (left colon cancer) in our hospital. Fifty healthy SPF Kunming mice were purchased from Liaoning Changsheng Biotechnology Co., Ltd. **Results:** The mRNA expression of miR-129-3p in the STC group was lower than that in the control group (CTLR) ($P < 0.05$). The mRNA expression of miR-129-3p in STC group was lower than that in the NC group ($P < 0.05$), and mRNA expression in STC+miR-129-3p group was higher than that in STC+miR-NC group ($P < 0.05$). In the first week, the weight of dry and wet feces of the STC group was lower than that of the NC mice ($P < 0.05$), and the weight of dry feces and wet feces of the STC group was lower than that of the NC group at the 2, 3, and 4 weeks, STC+miR-129-3p was higher than that in the STC group ($P < 0.05$). **Conclusion:** The increased expression of C-kit and SCF regulated by miR-129-3p contributed to the protection of interstitial cells. Knockdown of miR-129-3p expression could inhibit the activation of AKT/mTOR signaling pathway, reduce cell proliferation activity.

Keywords: miR-129-3p; SCF C-kit; STC; Autophagy; Apoptosis

Received: 07 September, 2021; **revised:** 10 January, 2022; **accepted:** 14 June, 2022; **available on-line:** 04 September, 2022

✉ e-mail: sdqchris2019@tmu.edu.cn

[#]These authors contributed equally to this paper.

Acknowledgements of Financial Support: This study was supported by National Science Foundation of China (No. 81770537 and 82070554).

Abbreviations: CCK-8, cell counting kit-8; GAPDH, Glyceraldehyde-3-phosphate dehydrogenase; ICC, interstitial cells of Cajal; PBS, phosphate buffered saline; SDS, sodium dodecyl sulfate; STC, slow transit constipation

INTRODUCTION

Constipation is a common functional gastrointestinal disease, which is characterized by persistent difficulty in defecation, few defecation times or incomplete defecation (Fuchs *et al.*, 2020). The prevalence rate of constipation in the world ranges from 0.7% to 81%, and the prevalence rate of constipation in the elderly is the highest. Slow transit constipation (STC) is a chronic and refractory common gastrointestinal disease, affecting 30%

of patients with chronic constipation in western countries, and the incidence of STC in young women is higher than that in men (Yates, 2020). STC causes intractable constipation, which has little response to conservative treatment and tends to be neurodegenerative diseases. For some patients with mild STC, constipation symptoms can be relieved only by high fiber diet (Hayashi *et al.*, 2021). However, patients with severe STC did not respond to dietary fiber or laxatives. At present, it has been proved that interstitial cells of Cajal (ICC) are related to the pathogenesis of constipation (Wang *et al.*, 2020). ICC is located between nerve endings and smooth muscle cells in gastrointestinal tract. ICC is generally considered as a pacemaker cell and a neuromuscular transmission medium of gastrointestinal activity. Studies have shown that ICC density in colon of patients with slow transit constipation is significantly lower than that of normal patients (Huang *et al.*, 2018). Therefore, the decrease of ICC may lead to the lack of slow wave activity, which affects the contraction response and leads to delayed transmission in patients with slow transit constipation. The maintenance of ICC requires SCF C-kit signal, which indicates that inhibiting this pathway can lead to the decrease of ICC number (Maestroni, 2020). This may lead to the development of STC. However, there is no investigation report on whether the decrease of ICC in STC patients is related to the inhibition of SCF C-kit signaling pathway. It is worth noting that although a variety of treatment management strategies have been formulated, including fiber supplements, prokinetic drugs and biofeedback therapy, total colectomy, and ileorectostomy are still the final and most effective treatment methods for STC patients (Boonhok *et al.*, 2021). In addition, STC overlaps with other constipation subtypes (including irritable bowel syndrome and pelvic floor dyssynergia), which highlights the complex mechanism involved in STC. Therefore, it is suggested to use more molecular biomarkers to treat STC, not just histopathological features. The participation of miRNA can provide an in-depth understanding of STC pathogenesis and treatment options. According to reports, miR-129-3p is a key miRNA related to the pathogenesis of STC (Bae & Kim, 2020). Autophagy is a cellular metabolic mechanism, which transports intracellular substances to lysosomes for degradation and promotes the synthesis of new substances. Autophagy disorder occurs in the pathogenesis of many diseases, including inflammation, neurodegenerative diseases, and cancer (Junejo *et al.*, 2020). Autophagy leads to slow wave rhythm and abnormal excitation conduction in gastrointestinal tract, which is the key mechanism of many gastrointestinal diseases including STC. Therefore, the study of ICCs from

autophagy is of great significance for understanding the pathogenesis of STC. The purpose of this study was to explore the mechanism of miR-129-3p affecting ICC autophagy in STC through SCF C-kit signaling pathway, and to provide new evidence for miRNA treatment of STC.

MATERIALS AND METHODS

Human body samples

The present study was approved by the Ethics Committee of Tianjin Medical University General Hospital (No. IRB2020-YX-123-01). Colon specimens were taken from 20 STC patients who received total colectomy plus rectocele anastomosis or subtotal colectomy plus antiperistalsis rectal anastomosis in our hospital. The control of this study was 20 patients who underwent radical operation for colon cancer (left colon cancer) in our hospital. These control patients had no constipation and no colon dilatation. A control specimen was obtained at least 5 cm away from the resection edge of the tumor-free area. Neither the study group nor the control group received any drugs that might increase the inflammatory infiltration of lamina propria or mucosa. Both STC group and control group used the same area.

Experimental mice

Fifty healthy Specific Pathogen Free (SPF) Kunming mice (6 weeks old, half of them male and half female) weighing 19 ± 3 g were purchased from Liaoning Changsheng Biotechnology Co., Ltd. (Liaoning, China). All animals were kept in a laboratory with a temperature of 20–25°C and a relative humidity of 40–60% under a 12-hour light/dark cycle. All mice were provided with common feed and drinking water at will. All experiments followed the nursing and use guidelines of laboratory animals in our hospital. The animal study has been approved by the ethics committee of Tianjin Medical University General Hospital (approval number: IRB2020-YX-123-01).

Experimental grouping

According to the experimental procedure and research purpose, human tissue samples were divided into control group NC (samples from patients undergoing radical operation for colon cancer, $n=20$) and STC group (samples from STC patients undergoing colon resection, $n=20$). The experimental mice were divided into NC (fed with normal saline water as experimental control, $n=15$), STC (STC model induced by intragastric administration of atropine 0.1 mg/kg and diphenoxylate 10 mg/kg, $n=15$), and STC+miR-NC (negative control of intravenous injection of miR-129-3p on the basis of STC, $n=15$). ICC cultured under normal conditions can be divided into CTRL (ICC cultured under normal conditions as experimental control), inhibitor NC (negative control of miR-129-3p silencing transfection), and miR-129-3p inhibitor (ICC transfected with miR-129-3p inhibitor).

STC model establishment and processing

The mouse STC model induced by atropine-diphenoxylate was established as described above, with some modifications. After adapting to the environment for one week, all mice except the control group (Montoya-Rosales *et al.*, 2016) were injected with atropine (0.1 mg/kg)

– diphenoxylate (10 mg/kg) once a day for 14 consecutive days. The miR-129-3p treated group (STC+miR-NC) was injected with miR-129-3p negative control through a tail vein, and the STC mice treated with miR-129-3p mimetic (STC+miR-129-3p) were injected with miR-129-3p suspended in 1 mL PBS through a tail vein at a dose of 100 µg.

ICC isolation and culture

Mice were killed by cervical dislocation. The large intestine of rats (from 2 cm below cecum to rectum) was taken out and opened along the mesenteric boundary. Cold phosphate buffered saline solution (PBS) (HyClone, USA) containing 2% antibiotics/antifungal agents (Beyotime, Shanghai) was used to remove the lumen contents, and the mucosa tissues were removed by acute dissection under dissecting microscope. Intestinal muscles (excluding mesentery and blood vessels) were equilibrated in digestive juice (pH 7.0, containing 1.3 mg/ml type II collagenase, Sigma, USA) at 37°C for 3 hours. Single cells were obtained by gently stirring in a centrifuge tube for 5 minutes, and the dispersed cells were filtered through a 200 µm filter. The dispersed cells were cultured in M199 growth medium (Gibco, USA) containing 10% fetal bovine serum (Gibco, USA) and 25 ng/mL mouse stem cell factor (Sigma, USA) in an incubator humidified by 5% CO₂ at 37°C. All experiments of ICC cluster were carried out after 72 hours of culture.

Cell transfection

The miR-129-3p inhibitor was purchased from Ribobio Corporation (Guangzhou, China). Lipofectamine 3000 reagent was used for cell transfection according to the manufacturer's instructions. QRT-PCR was performed to verify the transfection effect.

Reverse transcription polymerase chain reaction

Colon tissue and ICC were homogenized with Trizol. Total RNA (500 ng) was reverse transcribed into cDNA using PrimeScript RT Master Mix (Dalian, China). These procedures were strictly in accordance with the manufacturer's agreement. CDNA was amplified by ABI 7500 system using DNA binding dye SYBR Green. Glyceraldehyde-3-phosphate dehydrogenase (GAPDH) was used as an internal reference gene, and 2^{-ΔΔC_t} method was used to evaluate the change of mRNA expression.

Comparison of weighing mouse feces

Animal feces were collected and counted during the experiment. The wet weight of feces was recorded immediately after collection, and the dry weight of feces was recorded after drying in a drying oven for 3 hours, and the dry weight and wet weight of feces of experimental mice were compared.

Evaluation of intestinal pass rate

The intestinal transit rate was calculated as follows: intestinal transit rate (%) = $A/B \times 100\%$ (A: the length between the pyloric sphincter and the carbon-stained intestinal end; B: full length of intestine (distance from pylorus) rectum).

Western blot analysis

Colon tissue samples and ICC were homogenized and lysed in sodium dodecyl sulfate (SDS) polyacrylamide gel electrophoresis sample buffer. The mixture

was boiled and centrifuged at 12000 rpm for 20 minutes, and the supernatant was collected. An equal amount of protein (30 μ g) was separated from each sample on 10% SDS polyacrylamide gel, transferred to a polyvinylidene fluoride membrane and incubated with 5% bovine serum albumin for 1 hour. The membrane was probed with primary antibody at 4°C overnight. Next, the membrane was washed and incubated with horseradish peroxidase-linked secondary antibody. Enhanced chemiluminescence kit (Millipore) was used to detect immune response signals.

Determination of cell viability and apoptosis

The activity of ICC in different groups was estimated by cell counting kit-8 (CCK-8). In this study, flow cytometry (BD FACSVia) used a scattered-light gate, i.e., a combined FSC and SSC (lateral scattered-light) gate was more commonly used. Its biggest advantage is that it can eliminate the interference of debris or noise. The phylum cell population can be set according to the different cell distribution on the FSC *vs* SSC scatter plot. The number of cells detected by flow cytometry was 5000 per time.

Flow cytometry uses a threshold gate. FSC (Forward scattered light) is the most commonly used threshold parameter. FSC was positively correlated with cell size. By setting a threshold value with FSC, signals of other impurities such as cell debris below this threshold can not be processed. 1) Removal of cell debris: Establish a forward scattering (FSC) *vs*. A side-scattering (SSC) dot plot, and various photomultiplier tube devices are adjusted to ensure that all the cell populations to be analyzed are within the visual range of the dot plot. If necessary, the FSC threshold needs to be set and adjusted to exclude most of the cell debris, bubbles, and laser background noise from the analysis area (all should be located in the FSC-LOW area). Next, circle the area around the population of cells of interest (R1) in the FSC *vs* SSC point plot, which can be referred to as "R1-FSC *vs* SSC". Negative control: 2) to apply the appropriate fluorescence dye cell, it is recommended that you divide the cells in the two test tubes, one of the test tubes with fluorescently labeled antibodies dye cells of interest, and the other *in vitro* application type with fluorescent antibody as the corresponding negative control to help in the analysis for more accurate region of positive signals and negative fluorescence background. 3) Exclusion of dead cells: Cells are stained with markers such as Propidium Iodide (PI) or 7-AAD, which measure cell activity, to distinguish living cells from dead cells. First build the FSC *vs* "cell active staining" dot plot and then set "Region 1-FSC *vs* SSC" on this dot plot. The Viable cell population was then circled and called "Region 2-Viable". 4) If appropriate, the Viable was stained with a shared marker. In some cases, it was possible to dye a marker that was expressed both in the cell of interest and in other cells (such as CD45, which was expressed in all leukocytes). Although this step is not necessary, it can be helpful in analyzing some rare cell types. First, an FSC *vs* "shared marker" dot plot was established, and "Region 2-Viable" was set on the dot plot. Then, all cell populations expressing this Marker were circled and set as "Region 3-shared Marker". 5) Set up the necessary fluorescence analysis point map and apply the corresponding fluorescence homotype negative control to help distinguish the positive signal from the background fluorescence signal.

EdU incorporation analysis

The assay of 5-ethynyl-2'-Deoxyuridine (EdU) incorporation was carried out 48 hours after transfection according to the manufacturer's instructions using the Cell-Light EdU Apollo567 *in vitro* imaging kit (RiboBio, Guangzhou, China). The image was taken under a fluorescence microscope.

Statistical analysis

The normality of data distribution and the homogeneity of variance was tested. The data in this study are all SPSS 20.0 statistical analysis software. Firstly, the normality of the data is detected. The data of this study is in line with the normal distribution; The measurement data are expressed by mean \pm standard deviation (\pm S.D.), the inter group comparison adopts one-way ANOVA or repeated measurement ANOVA, and the inter group comparison adopts LSD-*t* test; The counting data were expressed as percentage (%), and the comparison between groups was expressed as percentage (%) χ^2 analysis; $P < 0.05$ means the difference is statistically significant.

RESULTS

The expression of miR-129-3p in colon tissue of STC patients decreased

The expression of miR-129-3p in tissue samples was analyzed by qRT-PCR. The expression of miR-129-3p in STC group was lower than that in CTRL group ($P < 0.05$). The data showed that the expression of miR-129-3p in colon tissue of STC patients was lower (Fig. 1).

Note: the mRNA expression of miR-129-3p in STC group was lower than that in CTRL group ($P < 0.05$). The data showed that the expression of miR-129-3p in colon tissue of STC patients was lower.

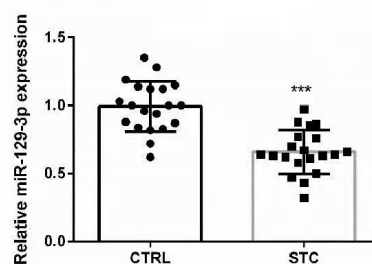


Figure 1. qRT-PCR analysis of miR-129-3p expression

Note: the mRNA expression of miR-129-3p in STC group was lower than that in CTRL group.

mRNA expression analysis of miR-129-3p in experimental mice

The mRNA expression of miR-129-3p in STC group was lower than that in NC group ($P < 0.05$), while the mRNA expression of STC+miR-129-3p group was higher than that of STC+miR-NC group ($P < 0.05$) (Fig. 2).

Note: the mRNA expression of miR-129-3p in STC group was lower than that in NC group ($P < 0.05$), and the mRNA expression in STC + miR-129-3p group was higher than that in STC + miR-nc group ($P < 0.05$).

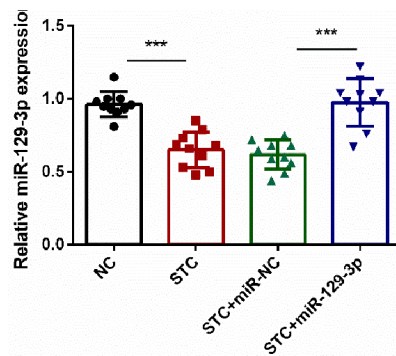


Figure 2. qRT-PCR analysis of miR-129-3p expression in mice
Note: the mRNA expression of miR-129-3p in STC group was lower than that in NC group, and the mRNA expression in STC+miR-129-3p group was higher than that in STC+miR-nc group

Comparative analysis of dry weight of mouse feces

The animal feces were collected and dried in a drying oven. Before the experiment (0 Week), there was no difference in the dry feces weight between the experimental groups ($P>0.05$). In the first week, the weight of dry feces and wet feces of the STC group was lower than that of the NC mice ($P<0.05$), and the weight of dry feces and wet feces of the STC group was lower than that of the NC group at the 2, 3, and 4 weeks, STC+miR-129-3p was higher than that in the STC group ($P<0.05$) (Table 1).

Note: before the experiment (0 week), there was no difference in the weight of dry feces among the experimental groups ($P>0.05$). The weight of dry feces in STC group was lower than that in NC group ($P<0.05$). At 2 week, 3 week and 4 week, the weight of dry feces in STC group was lower than that in NC group, and STC + miR-129-3p was higher than that in STC group ($P<0.05$).

Comparative analysis of wet weight of mouse feces

The wet feces of animals were collected and weighed immediately. Before the experiment (0 week), there was

Table 1. Weighing analysis of dry feces of mice (s)

Group	0 Week	1 Week	2 Week	3 Week	4 Week
NC	1.82±0.24	2.18±0.28	2.40±0.34	2.46±0.33	2.18±0.26
STC	1.92±0.25	1.93±0.30	1.77±0.27	1.61±0.24	1.92±0.22
STC+miR-NC	1.90±0.23	2.08±0.26	1.55±0.23	1.66±0.23	1.91±0.23
STC+miR-129-3p	2.01±0.22	2.03±0.25	1.80±0.22	1.96±0.23	2.01±0.25
<i>F</i> value	14.026	11.583	13.299	13.205	9.145
<i>P</i> value	0.024	0.015	0.005	0.011	0.004

Table 2. Weighing analysis of wet feces of mice (s)

Group	0 Week	1 Week	2 Week	3 Week	4 Week
NC	65.73±5.14	64.42±5.01	71.88±6.38	63.33±5.24	71.65±6.10
STC	62.51±4.27	52.19±3.14	56.67±3.16	50.91±3.15	53.75±3.88
STC+miR-NC	70.3±2.44	47.36±4.82	44.71±3.55	59.62±3.77	62.11±3.64
STC+miR-129-3p	58.82±3.44	63.13±5.81	56.28±5.36	77.01±5.66	66.69±3.41
<i>F</i> value	14.025	11.526	10.025	11.414	12.683
<i>P</i> value	0.172	0.022	0.015	0.031	0.026

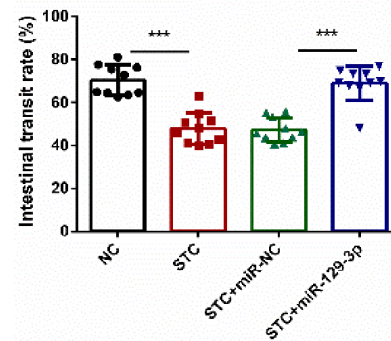


Figure 3. Intestinal passage rate of mice
Note: The intestinal passage rate of STC group and STC+miR-nc group was lower than that of NC group, and the intestinal passage rate of STC+miR-129-3p group was higher than that of STC group and STC+miR-nc group.

no difference ($P>0.05$). The feces weight of STC group and STC+miR-NC group was lower than that of NC group ($P<0.05$), and STC+miR-129-3p was higher than that of STC group and STC+miR-NC group (Table 2).

Note: before the experiment (0 week), there was no difference in the fecal weight of mice in each experimental group ($P>0.05$). The fecal weight of mice in 1week ~ 4 week STC group and STC+miR-nc group was lower than that in NC group ($P<0.05$), and the fecal weight of mice in STC+miR-129-3p was higher than that in STC group and STC+miR-nc group.

Effects of miR-129-3p on intestinal passage rate in mice

The intestinal passage rate was analyzed by calculating the proportion of the length between the pyloric sphincter and the end of the charcoal-stained intestine in the rectum. The intestinal passage rate of STC group and STC+miR-NC group was lower than that of NC group ($P<0.05$), while that of STC+miR-129-3p group was higher than STC group and STC+miR-NC group ($P<0.05$). The data showed that miR-129-3p could pro-

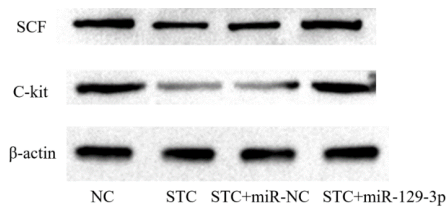


Figure 4. western blot analysis of SCF and C-kit expression

Note: The protein level of SCF and c-kit in STC+miR-nc group and STC group was lower than that in NC group, the protein level of SCF and c-kit in STC+miR-nc group and STC group was higher than that in STC+miR-nc group and STC group.

Table 3. Western blot analysis of SCF and C-kit expression (s)

Group	SCF	C-kit
NC	1.01±0.03	1.02±0.04
STC	0.51±0.01	0.45±0.01
STC+miR-NC	0.64±0.01	0.44±0.01
STC+miR-129-3p	0.88±0.02	0.92±0.03
F value	12.304	11.619
P value	0.004	0.012

mote intestinal peristalsis and improve the symptoms of constipation (Fig. 3).

Effects of miR-129-3p on SCF and C-kit protein level in STC mice

The expression of SCF and C-kit in colon tissue was analyzed by western blot. The protein level of SCF and C-kit in STC+miR-NC group and STC group was lower than that in NC group ($P<0.05$), while that in STC+miR-129-3p was higher than that in STC+miR-NC and STC group ($P<0.05$). High expression of miR-129-3p promoted the expression of SCF and C-kit in mouse colon (Fig. 4, Table 3).

Effect of miR-129-3p on SCF and C-kit mRNA expression in STC mice

The mRNA expression of SCF and C-kit in colon tissue of mice was analyzed by qRT-PCR. The mRNA expression of SCF and C-kit in STC group and STC+miR-NC group was lower than that in NC group ($P<0.05$). The mRNA expression of SCF and

Table 4. qRT-PCR analysis of SCF and C-kit expression (s)

Group	SCF	C-kit
NC	0.96±0.02	1.17±0.05
STC	0.63±0.01	0.7±0.02
STC+miR-NC	0.53±0.01	0.61±0.02
STC+miR-129-3p	0.88±0.02	1.00±0.04
F value	10.583	12.667
P value	0.024	0.008

Table 5. Analysis of miR-129-3p mRNA (s) in ICCs by QRT-PCR

Group	miR-129-3p mRNA
CTRL	0.95±0.03
inhibitor NC	0.89±0.03
miR-129-3p inhibitor	0.38±0.01
F value	10.673
P value	0.006

C-kit in STC+miR-129-3p group was higher than that in STC+miR-NC group and STC group ($P<0.05$) (Table 4).

qRT-PCR analysis of miR-129-3p mRNA in ICCs

The expression of miR-129-3p mRNA in ICCs was analyzed by RT-PCR. The expression of miR-129-3p mRNA in inhibitor group was lower than that in inhibitor NC and CTRL group ($P<0.05$), which indicated that miR-129-3p transfection was successful (Table 5).

The effect of knocking down miR-129-3p on ICC cell proliferation

The proliferation activity of ICC cells was detected by EDU infiltration method and CCK-8. The experimental data showed that compared with inhibitor NC and CTRL groups, the proliferation and viability of ICC cells decreased ($P<0.05$), and the apoptosis rate increased ($P<0.05$), which indicated that knocking down miR-129-3p inhibited the proliferation of ICC cells and promoted apoptosis (Fig. 5).

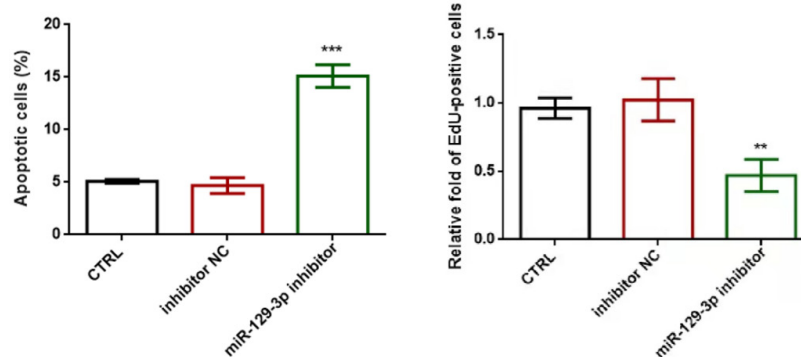


Figure 5. Analysis of apoptosis and proliferation

Note: The experimental data showed that compared with inhibitor NC and CTRL groups, the proliferation and viability of ICC cells decreased ($P<0.05$), and the apoptosis rate increased ($P<0.05$)

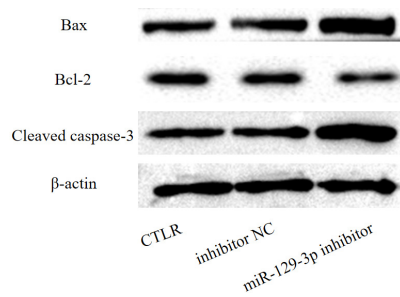


Figure 6. Western blot analysis of expression of apoptosis-related proteins

Note: The expression of Bax and Cleaved caspase-3 in miR-129-3p inhibitor group was higher than that in inhibitor NC and CTLR group, while the expression of Bcl-2 was lower.

Table 6. Western blot analysis of expression of apoptosis-related proteins (s)

Group	Bax	Bcl-2	Cleaved caspase-3
CTLR	0.94±0.06	0.98±0.08	0.91±0.06
inhibitor NC	0.96±0.08	0.97±0.06	1.07±0.08
miR-129-3p inhibitor	1.97±0.11	0.55±0.03	1.81±0.12
<i>F</i> value	14.527	9.324	13.891
<i>P</i> value	0.004	0.011	0.005

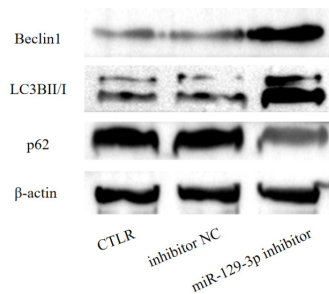


Figure 7. Expression analysis of autophagy-related proteins

Note: The expression of Beclin1 and LC3BII/I in miR-129-3p inhibitor group was higher than that in inhibitor NC and CTLR groups, while the expression of p62 protein was lower.

Table 7. Expression analysis of autophagy-related proteins (s)

Group	Beclin1	LC3BII/I	p62
CTLR	0.96±0.08	0.89±0.06	0.98±0.06
inhibitor NC	1.01±0.10	0.96±0.08	1.02±0.08
miR-129-3p inhibitor	2.12±0.13	2.37±0.15	0.50±0.01
<i>F</i> value	10.728	13.146	12.853
<i>P</i> value	0.026	0.019	0.014

The effect of knocking down miR-129-3p on the expression of apoptosis-related proteins in ICC

The expression of Bax, Bcl-2, and Cleaved caspase-3 in ICC cells was analyzed by western blot. The expression of Bax and Cleaved caspase-3 in miR-129-3p inhibitor group was higher than that in inhibitor NC and

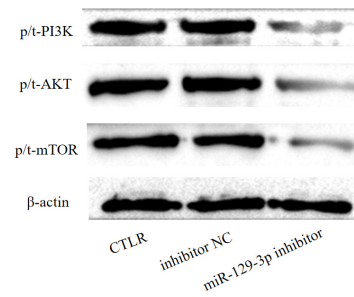


Figure 8. protein analysis of Akt/ mTOR signaling pathway

Note: The protein level of miR-129-3p inhibitor was lower than that of CTLR group.

Table 8. Protein analysis of Akt/ mTOR signaling pathway (s)

Group	p/t-PI3K	p/t-AKT	p/t-mTOR
CTLR	0.96±0.08	1.20±0.09	1.07±0.08
inhibitor NC	1.17±0.08	1.12±0.08	1.10±0.08
miR-129-3p inhibitor	0.40±0.01	0.54±0.01	0.41±0.01
<i>F</i> value	10.553	14.372	11.093
<i>P</i> value	0.006	0.025	0.017

CTLR group ($P<0.05$), while the expression of Bcl-2 was lower ($P<0.05$) (Fig. 6, Table 6).

Knocking down miR-129-3p promoted autophagy of ICC cells

The expression of autophagy-related proteins Beclin1, LC3BII/I, and p62 was analyzed by western blot. The expression of Beclin1 and LC3BII/I in miR-129-3p inhibitor group was higher than that in inhibitor NC and CTLR groups ($P<0.05$), while the expression of p62 protein was lower ($P<0.05$) (Fig. 7, Table 7).

Knocking down miR-129-3p inhibited the activation of AKT/mTOR signaling pathway

The expression of AKT/mTOR signaling pathway in ICC was analyzed by western blot. The protein level of miR-129-3p inhibitor was lower than that of CTLR group ($P<0.05$). The results showed that knocking down miR-129-3p inhibited AKT/mTOR signaling pathway (Fig. 8, Table 8).

DISCUSSION

In this study, we proved that the high expression of miR-129-3p can effectively promote defecation and colon activity in STC model induced by atropine and diphenoxylate in mice. This was mediated by up-regulating the expression of SCF C-kit signaling pathway and promoting ICC activity. In ICC culture, knocking down miR-129-3p can increase the autophagy level of cells. Western blot analysis showed that the expression of Beclin1 and LC3BII/I in miR-129-3p inhibitor increased, while the expression of p62 decreased, indicating that autophagy was enhanced. This was also the reason for the decline of cell proliferation and cell viability. At the same time, it was found that this regulation was completed by affecting Akt/mTOR signaling pathway. Protein analysis of apoptosis factors showed that the expression of Bax and Cleaved Caspase-3 increased, and the expression of anti-apoptosis factor Bcl-2 decreased in miR-129-3p in-

hibitor, which fully indicated that miR-129-3p expression regulated ICC autophagy level, and then affected cell proliferation and apoptosis. The mRNA expression level of miR-129-3p decreased in human tissue samples and STC models of mice, which indicated that miR-129-3p was closely related to the STC.

The decrease in the number and viability of ICC cells is related to the pathogenesis of many human diseases, such as chronic unexplained nausea and vomiting, small intestinal obstruction, streptozotocin-induced diabetes, and gastric dysrhythmia in STC (Li *et al.*, 2021; Mawani *et al.*, 2019; Kawahara *et al.*, 2021; Kim *et al.*, 2020; Yu *et al.*, 2020; Cangemi *et al.*, 2019). ICC plays an important role in regulating intestinal movement by acting as a pacemaker for gastrointestinal muscles (De Pablo-Fernandez *et al.*, 2019). The maintenance of ICC phenotype and function in gastrointestinal system depends largely on signal cascade, which is mediated by the expression of tyrosine kinase receptor C-kit protein on cell surface (Yan *et al.*, 2020). Previous reports have shown that C-kit is a specific marker of ICC. Studies have shown that ICC cells and stem cell factors (SCF) are closely related to the C-kit/SCF signaling pathway (Xu *et al.*, 2018). SCF is the natural ligand of C-kit, which is expressed in various tissues of the body, but mainly produced by stromal cells in bone marrow (Chen *et al.*, 2021). C-kit is a transmembrane protein. It promotes the development and differentiation of ICC and maintains its normal physiological function (Barroso-Chinea *et al.*, 2020). C-kit labeling indirectly reflects the quantity and density of ICC. There are two isoforms of SCF, namely soluble SCF (sSCF) and membrane-bound SCF (mSCF), which are important to ICC function. However, mSCF has a more lasting effect on ICC (Cornet-Masana *et al.*, 2019). In addition to increasing the number of ICC, sSCF can partially reverse the pathological ICC changes in diabetic mice. Our study found that miR-129-3p can promote the activation of SCF C-kit signaling pathway, which proved that miR-129-3p can effectively inhibit the loss of ICC cells and the decrease of SCF C-kit expression in the pathogenesis of STC. Our use of ICC cells isolated from STC mice also directly showed that knocking down miR-129-3p can significantly reduce ICC proliferation activity. Therefore, we assumed that SCF C-kit pathway was damaged by STC, which led to the decrease of ICC, which may contribute to the etiology of STC. Previous studies have shown that miR-129-3p can affect Beclin-1 gene to inhibit autophagy (Liu *et al.*, 2019). Beclin-1 is the first effector identified in the initial stage of autophagy. It interacts with phosphatidylinositol 3-kinase to form a protein complex, which can recruit autophagy marker LC3 and start autophagy flow. In this study, it was found that knocking down miR-129-3p up-regulated Beclin-1 and lc3bii/I in ICC (Pan *et al.*, 2019). Autophagy is a highly conservative multi-step process, which is regulated by many autophagy-related genes. In autophagy network, mammalian target protein of rapamycin (mTOR) can be activated by phosphatidylinositol 3-kinase (PI3K) and serine/threonine kinase (Akt), thus inhibiting autophagy (Gao *et al.*, 2020). In this study, we studied ICC autophagy, Akt/mTOR signal and apoptosis, including an increase in autophagy, promoting apoptosis, and reducing the cell proliferation activity. And proved that miR-129-3p knockdown inhibited Akt/mTOR-related autophagy pathway, enhanced autophagy and enhanced Caspase-3-mediated ICC apoptosis.

CONCLUSION

To sum up, it was found that the increased expression of C-kit and SCF regulated by miR-129-3p was helpful to protect ICCs. Knocking down the expression of miR-129-3p could hinder the activation of SCF C-kit and AKT/mTOR signaling pathway, induce the increase of autophagy, promote apoptosis and reduce the cell proliferation activity, indicating that miR-129-3p was a key miRNA related to STC. At the molecular level, the mechanism of miR-129-3p participating in ICCs in STC was explored.

Declarations

Ethics approval and consent to participate. The study protocol was approved by the Ethics Committee of Tianjin Medical University General Hospital. Informed consent was obtained from all the study subjects before enrollment.

Consent for publication. Not applicable.

Availability of data and material. The datasets generated and analyzed during the current study are available from the corresponding author on reasonable request.

Competing interests. The authors declare that they have no competing interests.

Authors' contributions. BBR and DQS contributed to the conception and design of the study; JP and SQF performed the experiments, collected and analyzed data; HW, CXL and DQS wrote the manuscript; All authors reviewed and approved the final version of the manuscript.

Acknowledgements. None.

REFERENCES

- Bae SH, Kim MR (2020) Subtype classification of functional constipation in children: polyethylene glycol versus lactulose. *Pediatr Int* **62**: 816–819. <https://doi.org/10.1111/pecd.14235>
- Barroso-Chinea P, Luis-Ravelo D, Fumagallo-Reading F, Castro-Hernandez J, Salas-Hernandez J, Rodriguez-Nunez J, Febles-Casquero A, Cruz-Muros I, Afonso-Oramas D, Abreu-Gonzalez P, Moratalla R, Millan MJ, Gonzalez-Hernandez T (2020) DRD3 (dopamine receptor D3) but not DRD2 activates autophagy through MTORC1 inhibition preserving protein synthesis. *Autophagy* **16**: 1279–1295. <https://doi.org/10.1080/15548627.2019.1668606>
- Boonhok R, Sangkanu S, Norouzi R, Siyadatpanah A, Mirzaei F, Mitsunwan W, Charong N, Wisessombat S, Pereira M L, Rahmatullah M, Wilairatana P, Wiart C, Tabo HA, Dolma KG, Nissapatorn V (2021) Amoebicidal activity of *Cassia angustifolia* extract and its effect on *Acanthamoeba triangularis* autophagy-related gene expression at the transcriptional level. *Parasitology* **148**: 1074–1082. <https://doi.org/10.1017/S0031182021000718>
- Cangemi DJ, Flanagan R, Barshop K, Kuo B, Staller K (2019) Colonic stool burden a useful surrogate for slow transit constipation as determined by a radiopaque transit study. *Am J Gastroenterol* **114**: 519–523. <https://doi.org/10.14309/ajg.0000000000000149>
- Chen S, Liu L, Li Y, Li H, Sun X, Zhu D, Meng Q, Yao S, Du S (2021) Comparison of the effects of colonic electrical stimulation and prucalopride on gastrointestinal transit and defecation in a canine model of constipation. *Scand J Gastroenterol* **56**: 137–144. <https://doi.org/10.1080/00365521.2020.1856919>
- Cornet-Masana JM, Banus-Mulet A, Carbo JM, Torrente A, Guijarro F, Cuesta-Casanovas L, Esteve J, Risueno RM (2019) Dual lysosomal-mitochondrial targeting by antihistamines to eradicate leukaemic cells. *EBioMedicine* **47**: 221–234. <https://doi.org/10.1016/j.ebiom.2019.08.021>
- De Pablo-Fernandez E, Passananti V, Zarate-Lopez N, Emmanuel A, Warner T (2019) Colonic transit, high-resolution anorectal manometry and MRI defecography study of constipation in Parkinson's disease. *Parkinsonism Relat Disord* **66**: 195–201. <https://doi.org/10.1016/j.parkreldis.2019.08.016>
- Fuchs KH, Schulz T, Broderick R, Breithaupt W, Babic B, Varga G, Horgan S (2020) Transanal hybrid colon resection: techniques and outcomes for benign colorectal diseases. *Surg Endosc* **34**: 3487–3495. <https://doi.org/10.1007/s00464-019-07126-w>

- Gao F, Zhang N, Wen JM, Li SJ, Zhang SG, Zhang BY, Dai YL, He RN, Huang YS, Yu QQ (2020) Establishment and potential mechanism of recurrent cystitis-induced overactive bladder-like model in female rats. *J Biol Regul Homeost Agents* **34**: 1465–1470. <https://doi.org/10.23812/20-09-L>
- Hayashi Y, Asuzu DT, Bardsley MR, Gajdos GB, Kvasha SM, Linden DR, Nagy RA, Saravanaperumal SA, Syed SA, Toyomasu Y, Yan H, Chini EN, Gibbons SJ, Kellogg TA, Khazaei K, Kuro OM, Machado Espindola Netto J, Singh MP, Tidball JG, Wehling-Henricks M, Farrugia G, Ordog T (2021) Wnt-induced, TRP53-mediated cell cycle arrest of precursors underlies interstitial cell of cajal depletion during aging. *Cell Mol Gastroenterol Hepatol* **11**: 117–145. <https://doi.org/10.1016/j.jcmgh.2020.07.011>
- Huang ZP, Qiu H, Yu BP (2018) Acute cholecystitis reduces interstitial cells of Cajal in porcine gallbladder through decreased mRNA synthesis. *Cell Physiol Biochem* **47**: 535–544. <https://doi.org/10.1159/000489987>
- Junejo SA, Geng H, Li S, Kaka AK, Rashid A, Zhou Y (2020) Superfine wheat bran improves the hyperglycemic and hyperlipidemic properties in a high-fat rat model. *Food Sci Biotechnol* **29**: 559–567. <https://doi.org/10.1007/s10068-019-00684-8>
- Kawahara H, Omura N, Akiba T (2021) The usefulness of preoperative evaluation for intractable slow transit constipation by computed tomography. *J Anus Rectum Colon* **5**: 144–147. <https://doi.org/10.23922/jarc.2020-065>
- Kim K, Jeon HJ, Bae SH (2020) Value of fluoroscopic defecography in constipated children with abnormal colon transit time test results. *J Neurogastroenterol Motil* **26**: 128–132. <https://doi.org/10.5056/jnm18201>
- Li T, Yan Q, Wen Y, Liu J, Sun J, Jiang Z (2021) Synbiotic yogurt containing konjac mannan oligosaccharides and *Bifidobacterium animalis* ssp. *lactis* BB12 alleviates constipation in mice by modulating the stem cell factor (SCF)/c-Kit pathway and gut microbiota. *J Dairy Sci* **104**: 5239–5255. <https://doi.org/10.3168/jds.2020-19449>
- Liu B, Xiao X, Zhou X, Zhou J, Lan L, Long X, Pan Y, Du M, Zhao X (2019) Effects of *Lactobacillus plantarum* CQPC01-fermented soybean milk on activated carbon-induced constipation through its antioxidant activity in mice. *Food Sci Nutr* **7**: 2068–2082. <https://doi.org/10.1002/fsn3.1048>
- Maestroni GJM (2020) Adrenergic modulation of hematopoiesis. *J Neuroimmune Pharmacol* **15**: 82–92. <https://doi.org/10.1007/s11481-019-09840-7>
- Mawani M, Azeem A, Gheewala S, Butt N, Abid S (2019) Understanding constipation: A cross-sectional study from a developing country setting. *J Coll Physicians Surg Pak* **29**: 284–286. <https://doi.org/10.29271/jcpsp.2019.03.284>
- Montoya-Rosales A, Castro-García P, Torres-Juarez F, Enciso-Moreno JA, Rivas-Santiago B (2016) Glucose levels affect IL-37 expression in monocyte-derived macrophages altering the Mycobacterium tuberculosis intracellular growth control. *Microb Pathog* **97**: 148–153. <https://doi.org/10.1016/j.micpath.2016.06.002>
- Pan XL, Zhou L, Wang D, Han YL, Wang JY, Xu PD, Zhang HX, Zhou L (2019) Electroacupuncture at “Zusanli”(ST36) promotes gastrointestinal motility possibly by suppressing excessive autophagy via AMPK/ULK1 signaling in rats with functional dyspepsia. *Zhen Ci Yan Jiu* **44**: 486–491. (in Chinese) <https://doi.org/10.13702/j.1000-0607.180571>
- Wang Y, Shuang L, Yujie S, Xiaohui M, Wei W, Jidong W (2020) Activin A overexpression promotes rat follicular development through SCF-kit-mediated cell signals. *Gynecol Endocrinol* **36**: 1070–1073. <https://doi.org/10.1080/09513590.2020.1736026>
- Xu J, Xu H, Yu Y, He Y, Liu Q, Yang B (2018) Combination of luteolin and solifenacin improves urinary dysfunction induced by diabetic cystopathy in rats. *Med Sci Monit* **24**: 1441–1448. <https://doi.org/10.12659/msm.904534>
- Yan S, Yue YZ, Sun MM, Wu BS, Wang XP (2020) Suppressive effect of *Aurantii fructus immaturus* and *Atractylodis macrocephalae rhizoma* on glutamic acid-induced autophagy of interstitial cells of Cajal. *J Integr Med* **18**: 334–343. <https://doi.org/10.1016/j.joim.2020.04.005>
- Yates A (2020) Transanal irrigation: is it the magic intervention for bowel management in individuals with bowel dysfunction? *Br J Nurs* **29**: 393–398. <https://doi.org/10.12968/bjon.2020.29.7.393>
- Yu C, Zang L, Feng B, Zhang L, Xue P, Sun J, Dong F, Ma J, Zheng M (2020) Coexpression network analysis identified specific miRNAs and genes in association with slowtransit constipation. *Mol Med Rep* **22**: 4696–4706. <https://doi.org/10.3892/mmr.2020.11568>